Guided-mode absorption in ultrathin organic photovoltaics

Yutong Pang,[1,2] Nanditha Dissanayake,[2] and Matthew D. Eisaman[2]

[1]Physics Department, Stony Brook University, Stony Brook, NY, 11794
[2]Sustainable Energy Technologies Department, Brookhaven National Laboratory, Upton, NY, 11973

***Abstract* — We introduce a novel organic photovoltaic (OPV) design, termed a "slot OPV", that applies the principles of slot waveguides to confine light within the ultrathin (< 50 nm) active layer of an OPV. Our calculations demonstrate that a "slot OPV" can be designed with guided-mode absorption for a 10 nm thick active layer equal to the absorption of normal incidence on an OPV with a 100 nm thick active layer. These results, together with the expected improvement in charge extraction for ultrathin layers, suggest that "slot OPVs" can be designed with greater power conversion efficiency than today's state-of-the-art OPV architectures.**

***Index Terms* — optical waveguides, organic photovoltaics, photovoltaic cells, thin films.**

I. Introduction

Organic photovoltaics (OPVs) hold promise as a low-cost, highly scalable and sustainable photovoltaic technology, but significant increases in device performance are needed for economic viability [1], [2]. The conversion efficiency of OPVs has been limited due to the combined charge-extraction challenges of short exciton diffusion length (~10 nm in organic polymers), bimolecular recombination, and disorder-induced low free carrier mobility [1], [3]-[6].

While an ultrathin (< 50 nm) active layer is desirable to overcome the above challenges, the optical absorption for normal incidence decreases significantly for active layer thicknesses on the order of the exciton diffusion length [7]. Recent work suggests the possibility of achieving strong absorption in ultrathin active layers by efficiently scattering the incident light into guided optical modes [8] – [12].

An important question to ask is whether light trapping in guided modes can enable significant optical absorption for ultrathin OPVs. Guided modes are defined such that their electromagnetic fields in the top layer (cover) and bottom layer (substrate) of the waveguide decay exponentially with distance, thereby confining the energy in the waveguide structure [13],[14]. To this end, in this paper we calculate the fraction of incident power that can be absorbed by the active layer for each guided mode and for normally incident light in several OPV architectures. The primary purpose of this analysis is to determine the maximum possible absorption for each guided mode, and thereby determine whether light trapping via guided modes is a potentially promising approach for enabling ultrathin active-layer OPVs.

One goal of this investigation is to determine whether the optical absorption fraction (power absorbed in active layer/incident power) for guided modes of an OPV architecture with an ultrathin (< 50 nm) active layer can be equal to the absorption fraction of normal incidence on a "standard" OPV cell (glass / ITO / PEDOT:PSS / P3HT:PCBM (100 nm) / Al). Equivalent or improved optical absorption for a cell with ultrathin active layer compared to a standard cell, combined with the expected improvement in charge-extraction efficiency for the ultrathin cell [15], would enable ultrathin OPVs with overall improved power conversion efficiency compared to standard OPV cells. To this end, in this investigation, we are most interested in comparing the absorption fraction for guided modes in various OPV architectures to the absorption fraction of normally incident light in standard OPV cells.

We find that with judicious design of the optical properties of the various layers, the guided modes in OPVs can result in large absorption for ultrathin active layers. Specifically, we introduce a novel cell architecture that uses hole- and electron-transport layers with large refractive indices adjacent to the active layer to enable tight confinement of guided modes within ultrathin active layers. The underlying physics of this design is related to recent work on slot waveguides [16].

We note that this study is restricted to the calculation of the optical absorption of guided modes, and does not address the question of coupling to these modes, although recent work suggests that sufficient coupling to surpass the ray-optic light-trapping limit [17] can be achieved with a randomly textured surface [11]. The total power conversion efficiency for these modes relative to normal incidence will depend on the combined effects of optical absorption, coupling efficiency, and charge extraction relative to normally incident light. For example, if the absorption fraction of a specific guided mode in a cell with a 10 nm thick active layer cell is equivalent to the absorption fraction of normally incident light for a cell with a 100 nm thick active layer, the overall power conversion efficiency for the ultrathin cell will be higher than that for the thick cell only if the relative increase due to charge-extraction improvements is larger than the loss in optical absorption due to guided-mode coupling efficiency.

TABLE 1
OPTICAL CONSTANTS USED IN CALCULATIONS, ROUNDED TO NEAREST TENTH [22].

Material	300 nm		350 nm		400 nm		450 nm		500 nm		550 nm		600 nm		650 nm		700 nm		750 nm		800 nm	
	n	k	n	k	n	k	n	k	n	k	n	k	n	k	n	k	n	k	n	k	n	k
ITO	2.3	0.0	2.1	0.0	1.9	0.0	1.9	0.0	1.9	0.0	1.8	0.0	1.8	0.0	1.7	0.0	1.7	0.0	1.6	0.0	1.6	0.0
P3HT:PCBM	1.8	0.2	1.7	0.2	1.7	0.2	1.6	0.3	1.9	0.4	2.1	0.4	2.1	0.3	2.0	0.0	1.9	0.0	1.9	0.0	1.9	0.0
PEDOT:PSS	1.7	0.0	1.6	0.0	1.6	0.0	1.5	0.0	1.5	0.0	1.5	0.0	1.5	0.0	1.4	0.1	1.4	0.1	1.4	0.1	1.4	0.1
Al	0.3	3.6	0.4	4.3	0.5	4.9	0.6	5.5	0.8	6.1	1.0	6.7	1.2	7.3	1.5	7.8	1.9	8.3	2.4	8.6	2.7	8.5

II. METHODOLOGY

In order to compare guided-mode and normal-incidence absorption for various OPV structures, we need to calculate the electromagnetic field propagation within a multilayer structure like that shown in Fig. 1, both for the case of normally-incident light and for the case of guided modes. We use the Transfer Matrix Method (TMM) [13], [14] and Finite-Difference Time-Domain (FDTD - Lumerical Solutions, Inc.) to calculate the electromagnetic field distribution within the OPV structure for a given field incident upon the cell. We use

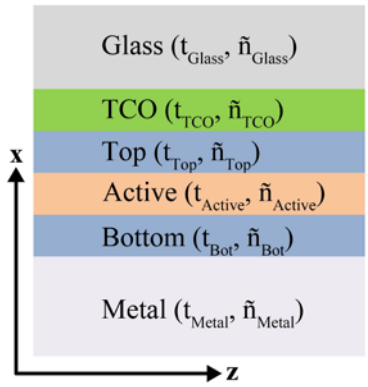

Fig. 1. Generic schematic of an OPV. Each layer has a thickness t, and a complex refractive index $\tilde{n} = n + ik$. TCO = Transparent Conductive Oxide and "Active" denotes the active layer intended for photon absorption.

TMM to solve for the guided modes of the OPV structure by obtaining the transfer equations, and solving these transfer equations to obtain the modal condition $X(\beta) = 0$, where β is the effective index of refraction, with the zeros of this equation corresponding to guided modes [13]. We solve this equation using Newton's method [18] in the complex plane. Once the effective index is known, this can be substituted back into our expression for the electric field using TMM or FDTD to calculate the electric field at any point in the structure for a given guided mode [19]. Once the electric field of each guided mode is known, we calculate the relative energy absorbed by each layer in the OPV structure. This allows us to calculate the fraction of light in a given guided mode that is absorbed by the active layer. The TE mode is distinguished by having the electric-field component E perpendicular to the plane of incidence, whereas, for TM mode, the magnetic field vector H is perpendicular to the plane of incidence [13].

We find that the calculations performed with TMM and FDTD agree with each other. For calculations presented in this paper, we explicitly state which method was used in each case.

Table 1 lists the values of the optical constants (real (n) and imaginary (k) part of the refractive index) used in our calculations. The optical constants of many of these materials depend on the deposition and processing conditions, and in practice may differ from those listed in Table 1.

III. RESULTS AND DISCUSSION

A. Standard OPV Structure

First, we determine the baseline optical absorption by calculating the absorption fraction for guided modes and normally incident light in the OPV structure shown in Fig. 1 with materials and thicknesses given by: glass/TCO (140 nm) / Top (40 nm) / Active (5 - 150 nm) / Metal (200 nm), where the TCO is indium tin oxide (ITO), the "Top" layer is poly(3,4-ethylenedioxythiophene):poly(styrenesulfonate) (PEDOT:PSS), the "Active" layer is poly(3-hexylthiophene):[6,6]-phenyl C_{61}-butyric acid methyl ester (P3HT:PCBM), the "Bottom" layer is absent, and the "Metal" layer is Al. The glass cover is treated as semi-infinite in our calculations. We shall refer to this structure as a "standard OPV" throughout the paper.

Figs. 2(a)-(c) show the fraction of light absorbed (at wavelengths λ=400 nm, 600 nm, and 800 nm, respectively) in the active layer of this standard OPV architecture for P3HT:PCBM active-layer thicknesses ranging from 5 nm - 150 nm. This calculation is performed for all guided modes that exist at a given thickness/wavelength combination, and also for normally incident light. At each active-layer thickness, the results shown in Fig. 2(a)-(c) are discretely integrated, from 300 nm to 800 nm with 50 nm wide bins, over the AM1.5G solar spectrum [20] to obtain the total absorption for each mode at a given active-layer thickness – this result is shown in Fig 2(d). We limit the upper wavelength of the integration to 800 nm because the absorption strength of P3HT: PCBM drops steeply at 650 nm, and is very small for wavelengths larger than about 650 nm. The TM_2 mode shown in Fig. 2(d) but not seen in Fig. 2(a)-(c) comes from the wavelength range 300 nm – 400nm. To obtain the plot shown

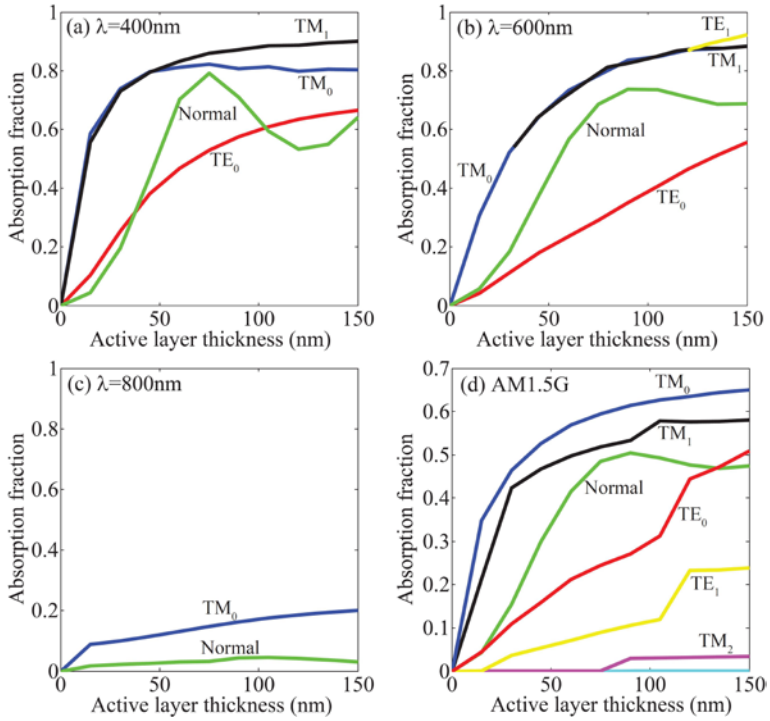

Fig. 2. Absorption fraction (power absorbed in active layer/incident power) vs. thickness of the active layer (P3HT: PCBM) for the "standard OPV" architecture (see text), for wavelength: (a) 400 nm, (b) 600 nm, (c) 800 nm, and (d) Average over AM1.5G solar spectrum [20]. Calculation performed using FDTD. For each guided mode, all the incident energy is assumed to be perfect coupled into the mode of interest. For normal incidence, the incident energy is the energy incident on the glass/ITO interface.

in Fig. 2(d), for a given active layer thickness, modes that exist over only part of the integration range of 300 nm – 800 nm are simply integrated over the part of the spectrum where they do exist.

From Fig. 2, we see that TM modes have a consistently larger absorption fraction than normal incidence, with the relative difference increasing greatly as the active layer thickness decreases. Fig. 2(d) shows that while the TM_0 absorption fraction asymptotically approaches 0.65 at an active layer thickness of 150 nm (a value approximately 1.4 times larger than that for normal incidence), at an active layer thickness of 10 nm, the TM_0 absorption fraction is approximately 8 times larger than that of normal incidence. This behavior makes physical sense, since for active layers thicker than about 100 nm, most of the normally incident light is absorbed and so less room for improvement exists by guiding modes in the active layer. For ultrathin active layers on the order of 10 nm thick, however, very little light is absorbed for normal incidence, meaning that any mode that is tightly confined to the active layer (such as TM_0 in this case) will have greatly enhanced absorption relative to the normal-incidence case. From Fig. 2(d), we see that a TM_0 guided mode in a standard OPV cell with a 40 nm-thick active layer will have the same absorption fraction as normal incidence on a standard cell with a 100 nm-thick active layer. An equivalent absorption fraction in a thinner active layer has the potential to result in an OPV with overall improved power conversion efficiency due to the improved charge extraction properties of the thinner active layers. As we shall see in the next section, the thickness of the active layer can be reduced even further with the optimization of the optical properties of the Top and Bottom hole- and electron-transport layers (see Fig. 1).

From Fig. 2 we also see that in contrast to the behavior of TM modes, the TE modes have absorption fractions that are less than or equal to the normal incidence case. The strong absorption of TM modes relative to TE modes is due to the stronger confinement of TM modes in the active layer of the cell for the standard OPV architecture. As we shall discuss in the next section, by carefully choosing the optical properties and thicknesses of the Top and Bottom hole- and electron-transport layers (see Fig. 1), the absorption fraction of both TM and TE modes can be increased by enabling tighter confinement of the guided mode in the active layer of the cell.

B. Ultrathin OPV with Embedded High-Index Layers

Recent investigations of so-called "slot waveguides" have demonstrated the strong confinement of light in layers on the order of 10 nm – 50 nm thick by sandwiching a thin relatively low-index layer between two layers of higher index [16]. We introduce a novel OPV design that applies the principles of

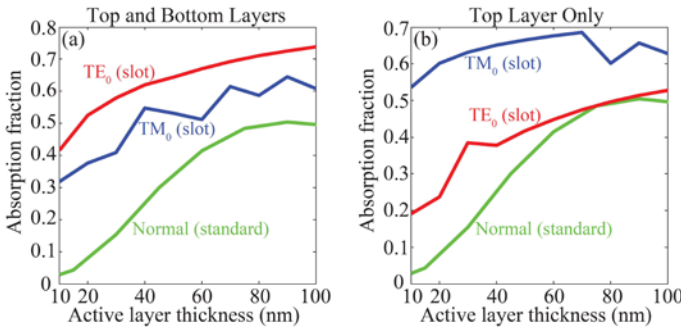

Fig. 3. Absorption fraction, averaged over the AM1.5G solar spectrum, of a slot OPV structure (glass/ITO/Top/P3HT:PCBM/ Bottom/Al) with: (a) $n_{Top}=n_{Bot}=3.5$, $k_{Top}=k_{Bot}=0$, and (b) $n_{Top}=3.5$, $k_{Top}=0$, and no Bottom layer. "TE_0 (slot)" and "TM_0 (slot)" refer to the guided modes in a slot OPV. "Normal (standard)" refers to normal incidence on a standard OPV (glass/ITO/PEDOT:PSS/ P3HT:PCBM/Al). The active-layer thickness is given by the x-axis. All calculations assume the following layer thicknesses: t_{glass}=semi-infinite, t_{ITO}=140 nm, t_{Top}=40 nm, t_{Bot}=40 nm, t_{Al}=200 nm.

slot waveguides to tightly confine light within the active layer of an ultrathin OPV structure. In terms of the generic schematic shown in Fig. 1, both the Top and Bottom hole- and electron-transport layers of such a structure have large values of refractive index relative to the active-layer index. We shall refer to this structure as a "slot OPV" throughout the paper.

Fig. 3(a) plots the absorption fraction of TE_0 and TM_0 guided modes averaged over the AM1.5G solar spectrum [20] as a function of active-layer thickness in the active layer of a slot OPV structure using t_{glass}=semi-infinite, t_{ITO}=140 nm, t_{Top}=40 nm, t_{active} = 10 nm -100 nm (x-axis of plot), t_{Bot}=40 nm, t_{Al}=200 nm, $n_{top} = n_{bot} = 3.5$, and $k_{top} = k_{bot} = 0$ (no absorption in Top and Bottom layers), and with the optical properties listed in Table 1. The absorption fraction is plotted as a function of active-layer thickness for guided modes (labeled "TE_0 (slot)" and "TM_0 (slot)") in this slot OPV structure, and normal incidence on the standard OPV studied in Fig. 2 (Top layer = PEDOT:PSS and no Bottom layer, labeled "Normal (standard)"). Fig. 3(b) assumes the same slot OPV structure as Fig. 3(a) except with no Bottom layer between the P3HT:PCBM active layer and the Al metal layer. For a given slot OPV design, an important metric for each mode is the active layer thickness required for that mode to have an absorption fraction equal to that of normal incidence on the "Normal (standard)" with 100 nm-thick active layer. Since charge extraction is expected to significantly improve for ultrathin active layers [1]–[3], an ultrathin slot OPV (t_{active} < 50 nm) with guided-mode optical absorption equal to the absorption of a "Normal (standard)" with t_{active} = 100 nm is expected to have significantly improved overall power conversion efficiency than state of art standard OPVs.

We first turn our attention to Fig. 3(a), which considers the case of Top and Bottom layers with $n_{Top}=n_{Bot}=3.5$, and $k_{Top}=k_{Bot}=0$. We see that the absorption fractions of the guided modes in a slot OPV are equal to the t_{active} = 100 nm absorption fraction of about 0.5 for the "Normal (standard)" case for a slot OPV active-layer thickness of (20 nm, 40 nm) for the (TM_0, TE_0) modes, respectively. This is a very important result, as it suggests that strong guided-mode absorption is possible for ultrathin active layers with thicknesses approaching the exciton diffusion length in these materials. Comparing this result to the guided-mode absorption for a standard OPV shown in Fig. 2(d), we see that the presence of the high-index Top and Bottom hole- and electron-transport layers adjacent to the active layer in the slot OPV case improves the absorption of the TM_0 and TE_0 modes in ultrathin active layers, with the improvement in the TE_0 mode being most pronounced. This may prove especially important from a practical perspective since the selective coupling of incident sunlight into TM modes is certainly less efficient than coupling into either TM or TE guided modes, as the slot OPV design allows.

From Fig. 3(b), we see that removal of the Bottom layer between the P3HT:PCBM and Al layers improves the absorption fraction of the TM_0 mode, but decreases that of the TE_0 mode. Specifically, the absorption of the guided modes in a slot OPV is equal to the "Normal (standard)" (t_{active} = 100 nm) absorption fraction of about 0.5 for a slot OPV active-layer thickness of (<10 nm, 90 nm) for the (TM_0, TE_0) modes, respectively. Figs. 3(a) and (b) demonstrate that is possible to equal or exceed the absorption of normally incident light on a "Normal (standard)" (t_{active} = 100 nm) cell with guided-mode absorption in an ultrathin "slot OPV".

The behavior observed in Fig. 3 can be understood by looking at Fig. 4, which plots the distribution of the square of the electric-field magnitude ($|E|^2$) for TE_0 (red) and TM_0 (TM_1 for 4(a)) (blue) modes at λ = 500 nm throughout a 10 nm-thick-active-layer slot OPV device. Fig. 4 considers a slot OPV with the structure: glass (semi-infinite, not shown) / ITO (140 nm) / Top (40 nm) / P3HT:PCBM (10 nm) / Bottom (40 nm) / Al (200 nm), for the case of: (a) $n_{Top}= n_{Bot}=3.5$; (b) $n_{Top}=3.5$, No Bottom layer, (c) $n_{Top}=1.8$, $n_{Bot}=1.8$, and (d) $n_{Top}=1.8$, No Bottom layer, with $k_{top} = k_{bot} = 0$ for all panels (a)-(d). The maximum value of $|E|^2$ for each plotted mode is normalized to 1. When one is using Fig. 4 ($|E|^2$) to help understand the results of Fig. 3 (absorption fraction in the active layer), it is important to remember that the absorption fraction of the active layer depends on electric field distribution in the layers, as well as the absorption strength of the active layer relative to other layers in the structure.

Fig. 4(a) shows that for $n_{Top}= n_{Bot}=3.5$, the TE_0 mode is mostly confined near the active layer, and due to the "slot-waveguide" effect, the TM_0 mode is tightly confined in the active layer [16]. This leads to strong absorption in active layer for both modes. As Fig. 4(b) shows, removing the Bottom Layer shifts the TE_0 mode away from the active layer and toward the Top layer, resulting in lower absorption than for the Top-and-Bottom-layer case in Fig. 4(a). This can also

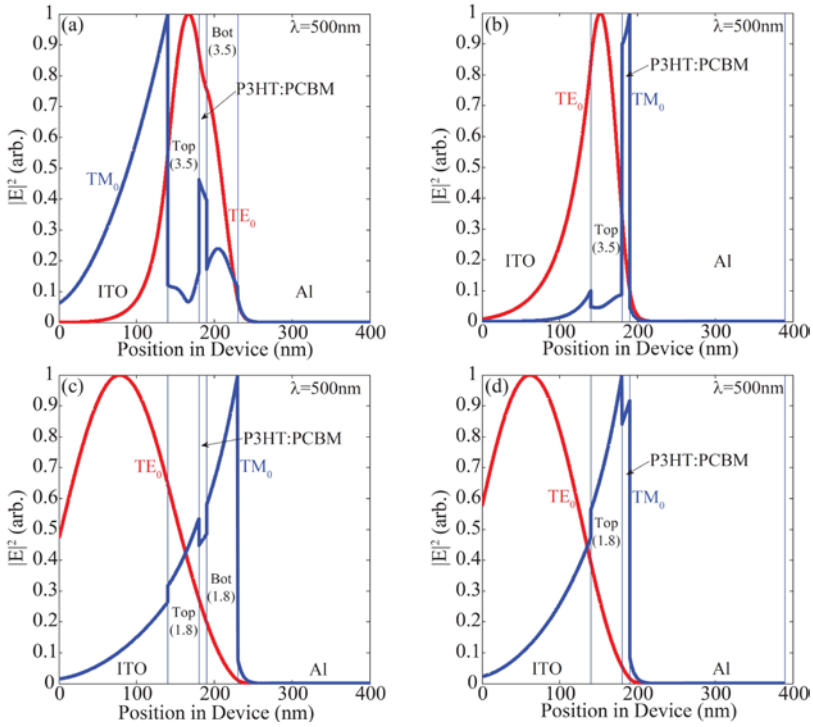

Fig. 4. Distribution of the electric field magnitude squared ($|E|^2$) at λ = 500 nm throughout a 10 nm-thick-active-layer slot OPV device – glass (semi-infinite, not shown) / ITO (140 nm) / Top (40 nm) / P3HT:PCBM (10 nm) / Bottom (40 nm) / Al (200 nm) - for the case of: (a) n_{Top}= n_{Bot}=3.5; (b) n_{Top}=3.5, No Bottom layer, (c) n_{Top}=1.8, n_{Bot}=1.8, (d) n_{Top}=1.8, No Bottom layer. k_{Top}= k_{Bot}=0 for all panels (a)-(d). Line colors are: Red=TE_0 guided mode, and Blue=TM_0 guided mode. Vertical lines show the separation between different layers in the cell. The maximum value of $|E|^2$ for each plotted mode is normalized to 1.

be seen by comparing the TE_0 mode absorption shown in Fig. 3(b) with that shown in Fig. 3(a). However, for the TM_0 mode in Fig. 4(b), we can see that removing the Bottom Layer leads to stronger active-layer confinement and stronger absorption than the Top-and-Bottom-layer case in Fig. 4(a). This can also be seen by comparing the TM_0 mode absorption shown in Fig. 3(b) with that shown in Fig. 3(a). The ideal configuration for a given application will depend on many factors, including the ability to couple selectively into specific modes such as TM_0, in which case a Top-Layer-Only design may be desired

Figs. 4(c) and (d) consider the cases of low-index Top and Bottom layers: (c) n_{Top}=1.8, n_{Bot}=1.8, and (d) n_{Top}=1.8, No Bottom layer, allowing us to understand the effect of reducing the real part of the refractive index. For the TE_0 mode, as the real parts of the refractive indices of the Top and Bottom layers decrease, the peak of the mode moves from the Top layer towards the ITO layer, resulting in decreased field amplitude in the active layer. For the TM_0 mode, as the real parts of the refractive indices of the Top and Bottom layers decrease, the confinement in the active layer weakens and even reverses. From this comparison, it is clear that the practical realization of ultrathin OPVs with improved power conversion efficiency will require high-index layers on either side of the active layer in order to enable sufficient optical confinement in the active layer. These high index layers may take the form of hole- and electron-transport layers as shown in Fig. 3(a), or a transport layer on one side and a metal electrode on the other side as shown in Fig. 3(b).

C. Experimental Tests

We have also performed preliminary experimental tests on the OPV architectures presented above. Prism coupling is an accurate method for the measurement of the effective index β of a given guided mode of a slab waveguide [21]. We used prism coupling to measure the effective index of the TE_0 mode at 633 nm for a "Standard" OPV cell with the structure glass / ITO (140 nm) / PEDOT (40 nm) / P3HT:PCBM (100 nm) / Ag (9 nm), with the prism contacting the Ag side of the cell. The measured value of β_{TE0}=1.63 agrees very well with the calculated values of β_{TE0}=1.63 (calculated with TMM) and β_{TE0}=1.62 (calculated with FDTD).

IV. Summary and Outlook

We calculated the fraction of energy absorbed by guided modes within ultrathin (active layer thickness < 50 nm) OPV structures, and compared this absorption to that obtained for normal incidence on a standard OPV (active layer thickness = 100 nm) in use today. We introduced a novel OPV design,

termed a “slot OPV”, that applies the principles of slot waveguides to tightly confine light within the active layer of an ultrathin OPV structure. Our calculations demonstrated that by judicious design of the layers and their optical properties, a “slot OPV” can be designed with a guided-mode absorption fraction for a 10 nm thick active layer that is equal to the absorption fraction of normal incidence on a “Standard OPV” with 100 nm thick active layer. These results, together with the expected improvement in charge extraction for ultrathin layers, suggest that ultrathin OPVs can be designed with greater overall power conversion efficiency than today’s state-of-the-art OPV architectures.

ACKNOWLEDGEMENT

We thank J. Jackson and L. Steingart for prism coupling measurements performed at Metricon Corp. This work was primarily performed at Brookhaven National Laboratory, and was partially supported by the U. S. Department of Energy, Sustainable Energy Technologies Department under contract DE-AC02-98CH10886.

REFERENCES

[1] G. Li, R. Zhu, and Y. Yang, “Polymer solar cells,” *Nature Photonics*, vol. 6, pp. 153−161, 2012.

[2] A. Mayer, S. Scully, B. Hardin, M. Rowell, and M. McGehee,“Polymer-based solar cells,” *Mater. Today*, vol. 10, 28–33, 2007.

[3] T. Kirchartz et al., “Efficiency limits of organic bulk heterojunction solar cells,” *J. Phys. Chem. C*, vol. 113, pp. 17958-17966, 2009.

[4] H. Hoppe and N. S. Sariciftci, “Organic solar cells: An overview,” *J. Mater. Res.*, vol. 19, pp. 1924−1945, 2004.

[5] L. J. A. Koster, E. C. P. Smits, V. D. Mihailetchi, and P. W. M. Blom, “Device model for the operation of polymer/fullerene bulk heterojunction solar cells,” *Phys. Rev. B*, vol. 72, p. 085205, 2005.

[6] M. Lenes, L. J. Koster, V. D. Mihailetchi, and P. W. Blom, “Thickness dependence of the efficiency of polymer:fullerene bulk heterojunction solar cells,” *Appl. Phys. Lett.*, vol. 88, p. 243502, 2006.

[7] Y. Zhang, R. Bekele et al., “Interdigitated bulk heterojunction organic photovoltaic cell with aligned copper phthalocyanine nanorodes,” *IEEE J. Sel. Top. Quant. Elect.*, vol. 16, pp. 1544−1551, 2010.

[8] P. Saeta et al., “How much can guided modes enhance absorption in thin solar cells?,” *Optics Express*, vol. 17, pp. 20975−20990, 2009.

[9] V. E. Ferry et al., “Light trapping in ultrathin plasmonic solar cells,” *Opt. Exp.*, vol. 18, p. A237, 2010.

[10] Z. Yu, A. Raman, and S. Fan, “Fundamental limit of nanophotonic light trapping in solar cells,” P*roc. Natl. Acad. Sci. U. S. A.*, vol. 107, pp. 17491−17496, 2010.

[11] D. M. Callahan, J. N. Munday, and H. A. Atwater, “Solar cell light trapping beyond the ray optic limit,” *Nano Lett.*, vol. 12, pp.214−218, 2011.

[12] M. A. Green, “Enhanced evanescent mode light trapping in organic solar cells and other low index optoelectronic devices,” *Prog. Photovolt: Res. Appl.*, vol. 19, pp. 473−477, 2011.

[13] J. Chilwell and I. Hodgkinson, “Thin-films field transfer matrix theory of planar multilayer waveguides and reflection from prism-loaded waveguides,” *J. Opt. Soc. Am. A*, vol. 1, pp. 742−753, 1984.

[14] P. Yeh, *Optical Waves in Layered Media*, Wiley-Interscience, Hoboken, NJ, 2005

[15] H. J. Queisser, “Photovoltaic conversion at reduced dimensions,” *Physica E: Lowdimensional Systems and Nanostructures*, vol. 14, pp. 1-10, 2002.

[16] V. R. Almeida, Q. Xu, C. A. Barrios, and M. Lipson, “Guiding and confining light in void nanostructure,” *Opt. Lett.*, vol. 29, pp.1209−1211, 2004.

[17] E. Yablonovitch, “Statistical ray optics,” *J. Opt. Soc. Am.*, vol. 72, pp. 899−907, 1982.

[18] M. S. Kwon and S. Y. Shin, “Simple and fast numerical analysis of multilayer waveguide modes,” *Opt. Comm.*, vol. 233, pp.119−126, 2004.

[19] L. A. Petterson, L. S. Roman, and O. Inganas, “Modeling photocurrent action spectra of photovoltaic devices based on organic thin films,” *J. Appl. Phys.*, vol. 86, pp.487−496, 1999.

[20] National Renewable Energy Laboratory (NREL). (2012, May). Reference Solar Spectral Irradiance: Air Mass 1.5. [Online]. Available: http://rredc.nrel.gov/solar/spectra/am1.5/.

[21] P. K. Tien, R. Ulrich, and R. J. Martin, “Modes of propagating light waves in thin deposited semiconductor films,”*Appl. Phys. Lett.*, vol. 14, pp. 291-294, 1969.

[22] M. McGehee. (2012, May). TransferMatrix.zip/ Index_of_Refraction_library.xls. [Online]. Available: http://www.stanford.edu/group/mcgehee/transfermatrix/.